

The effect of weak magnetic photon emission from quark-gluon plasma

Jing-An Sun¹ and Li Yan^{1,2}

¹*Institute of Modern Physics, Fudan University, Handan Road 220, Yangpu District, Shanghai, 200433, China*

²*Key Laboratory of Nuclear Physics and Ion-beam Application (MOE), Fudan University, Shanghai 200433, China*

(Dated: February 28, 2023)

We propose a novel effect that accounts for the photon emission from a quark-gluon plasma in the presence of a weak external magnetic field. Although the weak magnetic photon emission from quark-gluon plasma only leads to a small correction to the photon production rate, the induced photon spectrum can be highly azimuthally anisotropic, as a consequence of the coupled effect of the magnetic field and the longitudinal dynamics in the background medium. With respect to a realistic medium evolution containing a tilted fireball configuration, the direct photon elliptic flow from experiments is reproduced. In comparison to the experimental data of direct photon elliptic flow, in heavy-ion collisions the magnitude of the magnetic field before 1 fm/c can be extracted. For the top energy of RHIC collisions, right after the pre-equilibrium evolution, $|eB|$ is found no larger than a few percent of the pion mass square.

Introduction.— The nature of high temperature quantum chromodynamics (QCD) is the major focus for the high-energy heavy-ion experiments carried out at Relativistic Heavy-Ion Collider (RHIC) and the Large Hadron Collider (LHC). In these facilities, quark-gluon plasma (QGP), a fluid with color degrees of freedom, has been created [1, 2]. Dynamical properties of QGP have been well studied in terms of the observed spectra of various particles. Quite remarkably, at the top energies of RHIC and the LHC, a large number of hadron observables were found compatible with the theoretical modeling of QGP using viscous hydrodynamics, even at a high precision level [3, 4].

Albeit its extreme success, hydrodynamical modeling cannot describe photon productions from heavy-ion experiments [5–7]. At the top RHIC energies, in the low p_T region, experimentally measured direct photon yields (*i.e.*, photon yields excluding those from hadron decays) exceed the current theoretical predictions [8]. More importantly, in experiments the spectrum of direct photons can be as azimuthally anisotropic as pions, with in particular a large elliptic flow v_2^{γ} [9, 10]. From the theoretical modeling, however, direct photons are expected more isotropic [11–14]. This is a consequence that photon radiations from QGP are dominantly from the early stages [11], during which momentum anisotropy has not been fully developed. The discrepancy in both yields and elliptic flow is often referred to as the “direct photon puzzle” (cf. [5, 6]).

In theoretical models, to incorporate a significant emission anisotropy for the direct photons is challenging. There have been many attempts. One such type of theories relies on the mechanism of increasing photon radiations from the later stages of the QGP system [13, 15].

The presence of an external magnetic field, on the other hand, provides an alternative solution. In high-energy heavy-ion collisions, as a consequence of the relativistic motion of ions, magnetic fields are generated with extremely strong field strength [16–19], with $|eB|/m_{\pi}^2$ reaches $O(10)$ at the top energies of RHIC and $O(10^2)$ at the LHC, where m_{π} is the pion mass. Although the

influence of strong magnetic fields has already driven a number of physical predictions of great interest [20–22], because the pre-equilibrium stage of the QGP, in which the magnetic field decays most drastically, is hardly conducting, magnetic fields are expected weak as the system starts to evolve hydrodynamically. For instance, at around 0.4 fm/c and in the center of the fireball, the residual strength of magnetic field can drop to $|eB|/m_{\pi}^2 \approx 0.01$ in a non-central AuAu collision at the top RHIC energy. Nonetheless, after the pre-equilibrium stage, the detailed evolution of the magnetic fields in QGP remains undetermined, owing to the lack of knowledge of the electrical properties of the QGP medium [23–29].

Regarding photon productions, strong magnetic field assumption has been considered [30–34], which indeed gives rise to anisotropic emission. For instance, the synchrotron radiation induced by a strong magnetic field presents naturally an elliptic mode [33]. Note that the strong magnetic field assumption would modify the theoretical description dramatically. Especially, when $|eB| \gg T^2$, magnetohydrodynamics should be taken into account, while when $\sqrt{|eB|} \gg gT$, effect of magnetic fields cannot be neglected in quark scatterings. With respect to the realistic QGP system, these conditions lead to a rough criterion: $|eB|/m_{\pi}^2 \sim O(1)$.

In this Letter, we focus on the hydrodynamic stage of a QGP evolution, during which only a weak external magnetic field, $|eB|/m_{\pi}^2 \ll 1$, remains along with the medium. In this weak field scenario, the bulk part of hydrodynamical modeling is not affected, whereas photon productions in QGP receive a small correction due to the magnetic field. This small correction, which we refer to as the effect of weak magnetic photon emission, results in a large anisotropy in the direct photon spectrum.

Weak magnetic photon emission.— Photons radiated from a thermalized QGP can be produced by $2 \rightarrow 2$ scattering processes among quarks and gluons ($1 + 2 \rightarrow 3 + \gamma$) [35]. In a kinetic theory approach, the production

rate is [13, 14]

$$\begin{aligned} \mathcal{R}^\gamma &= \frac{1}{2(2\pi)^3} \sum_i \int \frac{d^3\mathbf{p}_1}{2E_1(2\pi)^3} \frac{d^3\mathbf{p}_2}{2E_2(2\pi)^3} \frac{d^3\mathbf{p}_3}{2E_3(2\pi)^3} \\ &\quad \times (2\pi)^4 \delta^4(P_1 + P_2 - P_3 - P) |\mathcal{M}_i|^2 \\ &\quad \times f_1(P_1) f_2(P_2) [1 \pm f_3(P_3)] \\ &\approx \frac{40\alpha_s}{9\pi^2} \mathcal{L} f_q(P) I_c, \end{aligned} \quad (1)$$

where the summation is over the Compton and the quark-antiquark annihilation channels with respect to the scattering amplitudes $|\mathcal{M}_i|^2$, and f_1 , f_2 and f_3 are distribution functions of quarks and gluons, correspondingly. The last expression in Eq. (1) gives the rate in the small angle approximation [36], with \mathcal{L} a Coulomb logarithm, and $I_c = \int d^3\mathbf{p}/(2\pi)^3 [f_g + f_q]/p$ effectively characterizing the conversion between a quark-antiquark and a gluon in the thermalized QGP [37].

In the previous studies based on hydrodynamics, dissipative effects in the medium have been taken into account to the photon production [14]. These effects are introduced via viscous corrections to the the quark and gluon distribution functions, $\bar{f} = n_{\text{eq}} + \delta f$, where n_{eq} is the equilibrium distribution and the correction δf is linear in the shear or bulk viscosity. Analogously, a weak external electromagnetic field induces additional correction to the quark distribution function, $f_q = \bar{f}_q + f_{\text{EM}} = f_q + \delta f_q + f_{\text{EM}}$. At the leading order of $|eB|/T^2$, from a straightforward derivation in kinetic theory, one finds,

$$f_{\text{EM}} = \frac{c}{8\alpha_{\text{EM}}} \frac{\sigma_{\text{el}} n_{\text{eq}} (1 - n_{\text{eq}})}{T^3 p \cdot u} e Q_f F^{\mu\nu} p_\mu u_\nu, \quad (2)$$

where eQ_f indicates the corresponding electrical charge a quark, σ_{el} is the electrical conductivity and u_ν is flow four-velocity. Although Eq. (2) applies more generally to weak electro- and magnetic fields, in this Letter we only focus on the magnetic field components, $B_i = \epsilon_{ijk} F^{jk}$. Eq. (2) is consistent to the kinetic theory definition of charge current, $j_{\text{EM}}^i = \sigma_{\text{el}} E^i = \sum_f Q_f \int \frac{d^3\mathbf{p}}{(2\pi)^3 p^0} p^i f_{\text{EM}}$, from which, depending on the number of quark flavors considered, the constant c can be determined.

Accordingly, the photon production rate receives corrections due to the presence of a weak external electromagnetic field, $\mathcal{R}^\gamma = \bar{\mathcal{R}}^\gamma + \mathcal{R}_{\text{EM}}^\gamma$, with $\mathcal{R}_{\text{EM}}^\gamma$ linear in the field strength. The background rate $\bar{\mathcal{R}}^\gamma$, which is entirely determined by \bar{f} , has been applied previously to calculate photon productions in heavy-ion collisions. After a space-time integral with respect to the medium evolution, it leads to the photon invariant spectrum,

$$E_p \frac{d^3\bar{N}}{d^3\mathbf{p}} = \int_V \bar{\mathcal{R}}^\gamma(P, X) = \bar{v}_0 (1 + 2\bar{v}_2 \cos 2\phi_p), \quad (3)$$

where X contains the space-time dependence in terms of the proper time $\tau = \sqrt{t^2 - z^2}$, transverse coordinates x , y and space-time rapidity $\eta_s = \text{arctanh}(z/t)$. In this work, we take the beam axis along z , and x - z plane is the

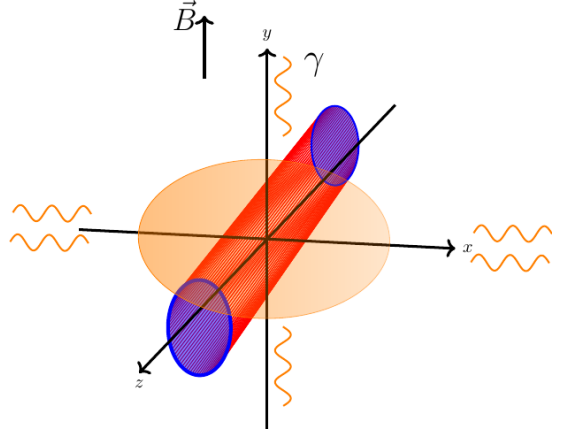


FIG. 1. A schematic demonstration of the weak magnetic photon emission: Photon radiations with an elliptic anisotropy induced by a weak external magnetic field on top of a tilted QGP fireball.

reaction plane. In Eq. (3) the Fourier decomposition of the invariant spectrum defines the direct photon yields \bar{v}_0 and elliptic flow \bar{v}_2 from the background, respectively. Similarly, one has for the corrections due to a weak magnetic field,

$$E_p \frac{d^3 N_{\text{EM}}}{d^3\mathbf{p}} = \int_V \mathcal{R}_{\text{EM}}^\gamma(P, X) = v_0^{\text{EM}} (1 + 2v_2^{\text{EM}} \cos 2\phi_p). \quad (4)$$

Here, v_0^{EM} and v_2^{EM} should be understood as the additional yields of photons and elliptic flow entirely associated with the corrections from the weak magnetic field. The final predictions of direction photon emissions are thereby

$$v_0^\gamma = \bar{v}_0 + v_0^{\text{EM}}, \quad v_2^\gamma = \frac{\bar{v}_2 \bar{v}_0 + v_2^{\text{EM}} v_0^{\text{EM}}}{\bar{v}_0 + v_0^{\text{EM}}}. \quad (5)$$

Let us now explain the effect of weak magnetic photon emission from QGP. In the weak magnetic field scenario, the magnetic field is too weak to modify the perturbative QCD scattering processes, but suffices to drive the medium slightly out of equilibrium. The shift in the momentum distribution of incoming quarks brings in an extra source of photon production on top of the $2 \rightarrow 2$ scatterings in both channels, which scales with temperature T as T^4 . Unlike the background contribution, where the photon elliptic flow is accumulated according to the space-time evolution of the azimuthal geometry of the medium, from the weak magnetic photon emission, v_2^{EM} is generated from two coupled effects: (1) A weak magnetic field which is orientated out of reaction plane. (2) Longitudinal dynamics of the background medium. Especially for the elliptic emission, one needs a rapidity-odd dipolar moment in the space-time geometry of the background medium. To show this, one first notices that the emitted photon spectrum are largely determined by the quark distribution function (cf., Eq. (1)), namely,

$\mathcal{R}_{\text{EM}}^\gamma \sim f_{\text{EM}}$. As shown in Fig. 1, with respect to a magnetic field out of reaction-plane, namely, $\vec{B} = B_y \hat{y}$, in the rate one expects from $F^{\mu\nu} p_\mu u_\nu \sim B_y p_x u_z \propto \cos \phi_p$. Therefore, to realize an elliptic emission which scales as $\sim \cos 2\phi_p$, an extra dipolar moment $\cos \phi_p$ in the background quark distribution is required. Fortunately, in heavy-ion experiments this dipolar moment has already been confirmed. In fact, in terms of the observed rapidity-odd directed flow v_1^{odd} [38–40] and rapidity-even dipolar flow v_1^{even} [41, 42] of charged hadrons, there exist both odd and even dipolar moments in the evolving medium. Because the direct photons are measured in a symmetric rapidity window, we concentrate on the odd dipolar moment in this work.

In Fig. 1, a schematic demonstration of the weak magnetic photon emission is shown with respect to a tilted fireball configuration, which contains a rapidity-odd dipolar moment in the background medium. In the Supplemental Material, the effect of the weak magnetic photon emission is verified in the case of Bjorken flow, where $v_2^{\text{EM}} = 0.5$.

Hydrodynamical modeling with weak magnetic photon emission.— In non-central heavy-ion collisions, the medium created by the colliding nuclei exhibits asymmetric distribution in the longitudinal direction, due to partly the structure of nucleus and partly the effect of longitudinal fluctuations. Effectively, the asymmetry in the medium can be captured in terms of a tilted fireball, based on which, hydrodynamical modeling reproduces the experimentally measured directed flow v_1^{odd} of charge hadrons [40].

Following Ref. [40], we take the initial entropy density distribution

$$s(\tau_0, \vec{x}_\perp, \eta_s) \propto w(\eta_s) [\chi N_{\text{coll}} + (1 - \chi)(N_{\text{part}}^+ w^+(\eta_s) + N_{\text{part}}^- w^-(\eta_s))], \quad (6)$$

where N_{coll} , N_{part}^+ and N_{part}^- are the densities of binary collisions and participants of the forward and backward going nuclei, respectively. As in the standard Glauber model, entropy production receives contributions from binary collisions and participants, relatively determined by the constant χ . Longitudinal description in Eq. (6) is introduced via the functions $w(\eta_s)$ and $w^\pm(\eta_s)$. The symmetric longitudinal profile,

$$w(\eta_s) = \exp\left(-\theta(|\eta_s| - \eta_M) \frac{(|\eta_s| - \eta_M)^2}{2\sigma_\eta^2}\right) \quad (7)$$

accounts for the longitudinal spectrum of charged hadrons, while

$$w^+(\eta_s) = \begin{cases} 0, & \eta_s < -\eta_T \\ \frac{\eta_T + \eta_s}{2\eta_T}, & -\eta_T \leq \eta_s \leq \eta_T \\ 1, & \eta_s > \eta_T \end{cases} \quad (8)$$

and $w^-(\eta_s) = w^+(-\eta_s)$ give rise to rapidity-odd component. For a given collision centrality, the spatial geometry

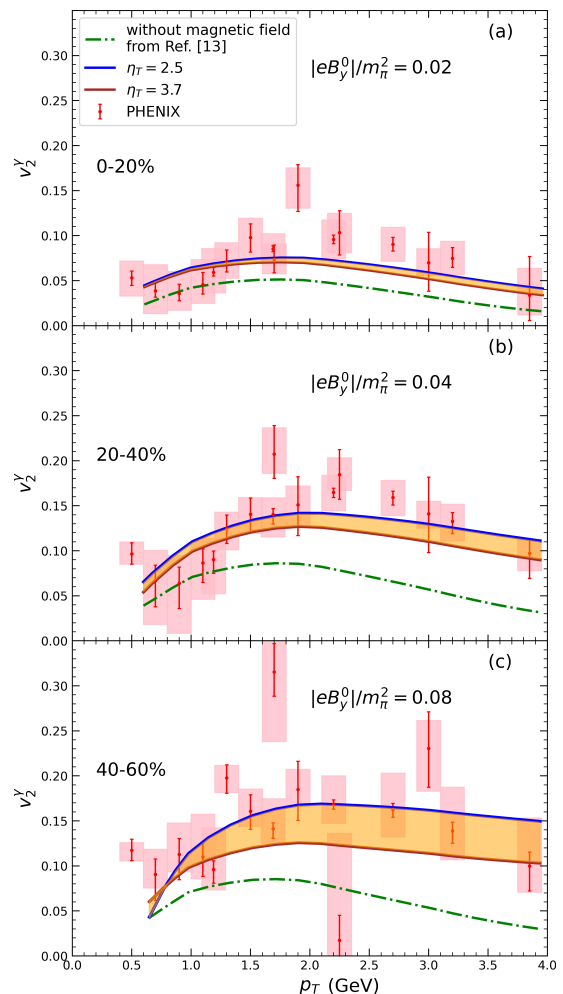


FIG. 2. Direct photon elliptic flow at RHIC at different centralities. Green dash-dotted lines are from hydrodynamical modeling without the effect of external magnetic field [13]. Final results with also weak magnetic photon emissions are shown as colored bands. Experimental data are from Ref. [9].

of the distribution relies entirely then on these parameters, η_T , η_M and σ_η , which we choose as in Ref. [40]. Note in particular, η_T determines the extent to which the fireball is tilted.

With respect to the initial condition Eq. (6), we solve 3+1 dimensional viscous hydrodynamics using the state-of-the-art MUSIC program [43, 44], which has also been used for the calculation of the background direct photon spectrum for \bar{v}_0 and \bar{v}_2 . To be consistent with the previous calculations in Ref. [13], we consider the weak magnetic photon emissions from QGP between initial time $\tau_0 = 0.4$ fm/c and an effective crossover temperature $T_c = 145$ MeV.

The evolution of the magnetic field along with the QGP medium contributes the most significant theoretical uncertainty to the predicted direct photon spectrum. In vacuum the fastest decay of the external magnetic field is expected, which is analytically solvable using the

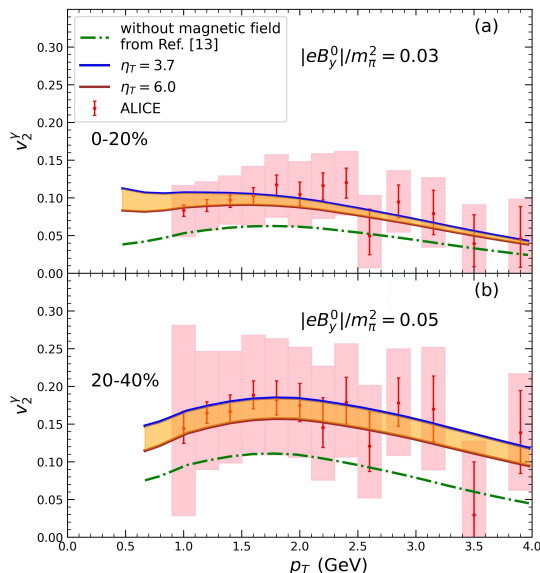


FIG. 3. Direct photon elliptic flow at LHC at different centralities. Green dash-dotted lines are from hydrodynamical modeling without the effect of external magnetic field [13]. Final results with also weak magnetic photon emissions are shown as colored bands. Experimental data are from Ref. [10].

Lienard-Wiechert potential with respect to the moving nuclei [22]. However, in the case of a conducting QGP, magnetic field in the medium could experience a much slower decay process. In order to verify the validity of the condition of weak magnetic photon emission, we consider the worst-case scenario with a space-time profile of the external magnetic field based on vacuum decay, $\Gamma(\tau, \eta_s)$, and neglect dependence on the transverse coordinates,

$$eB_y(\tau, \eta_s) = eB_y^0 \Gamma(\tau, \eta_s). \quad (9)$$

The profile is normalized, in a way that the parameter eB_y^0 identifies the field strength at initial time τ_0 and at $\eta_s = 0$. It should be emphasized that within this assumption, the effect of the external magnetic field is suppressed, and accordingly the parameter eB_y^0 only estimates the upper bound of field strength at initial time.

We will not calculate the direct photon spectrum \bar{v}_0 and elliptic flow \bar{v}_2 from the background medium directly, instead we extract them from the most updated hydrodynamical modeling in Ref. [13], where a variety of sources for photon emission have already been included. For instance, prompt photons produced from the initial hard scatterings are obtained via pQCD calculation at the NNLO order, photons from thermal radiations from QGP are calculated with respect to the $2 \rightarrow 2$ scattering amplitudes determined via pQCD at the leading-log order [45].

To separately calculate v_0^{EM} and v_2^{EM} , we consider u and d quarks that contribute to the photon emission. We take the small angle approximation for the photon

production rate [36, 46], with respect to the magnetic field induced correction to the quark distribution function f_{EM} in Eq. (2). To be consistent with the background calculations, we take the pQCD evaluation for the QGP electrical conductivity, $\sigma_{\text{el}}/T \approx 5.98$ [28, 45]. With respect to the QGP evolution characterized by hydrodynamical modeling for a tilted fireball condition, we find $v_2^{\text{EM}} \approx 0.6$, which is a bit larger than that from a simple Bjorken flow. Note that the value of v_2^{EM} does not depend on the magnitude of the magnetic field. Once v_0^{EM} and v_2^{EM} are given, the yields and the elliptic flow of direct photons in heavy-ion collisions can be obtained according to Eq. (5).

Direct photon v_2^{γ} .— In Fig. 2, the final results on the direct photon elliptic flow from RHIC AuAu collisions at $\sqrt{s_{NN}} = 0.2$ TeV are shown for the corresponding three centrality classes. Comparing to the background contributions (green lines), with the weak magnetic photon emissions, the elliptic flow of direct photons gets enhanced. Moreover, with the value of eB_y^0 properly chosen, the resulted model prediction reproduces the experimental data. By doing so, we are allowed to extract the value of eB_y^0 . We find that as centrality grows, the extracted value of eB_y^0 systematically increases, from $|eB_y^0| = 0.02m_\pi^2$ at the 0-20% centrality class, $|eB_y^0| = 0.04m_\pi^2$ at the 20-40% centrality class, to $|eB_y^0| = 0.08m_\pi^2$ at the 40-60% centrality class. All these values satisfy the weak magnetic field condition, $|eB|/m_\pi^2 \ll 1$. Weak magnetic photon emission leads to a minor increase in the direct photon yields, which in the centrality class 20-40%, is about 10%.

In Fig. 3, the direct photon elliptic flow are shown similarly for the PbPb collisions at $\sqrt{s_{NN}} = 2.76$ TeV. Comparing the RHIC data, there exist large experimental uncertainties from the LHC measurements. Nevertheless, with the effect of weak magnetic photon emissions, the resulted elliptic flow is improved significantly. Following the same strategy, we extract the value of eB_y^0 in the centrality classes 0-20% and 20-40%, leading to $|eB_y^0| = 0.03m_\pi^2$ and $|eB_y^0| = 0.05m_\pi^2$, respectively.

We also investigate the effect of the background dipolar moment by varying the parameter η_T . As in Ref. [40], we take η_T approximately between 40% of y_{beam} and $y_{\text{beam}} - 2.5$, so that the tilted fireball can capture the measured v_1^{odd} of charged hadrons. As expected, as shown as the colored bands in Fig. 2 and Fig. 3, the effect of weak magnetic photon emission is stronger with respect to a larger dipolar moment.

Summary and discussion.—We propose the weak magnetic photon emission as an extra source for photon productions from QGP. Although it only results in a small correction to the photon production rate, the resulted spectrum can be highly anisotropic, due to the coupled effect of a weak magnetic field and a non-trivial longitudinal dynamics of the background QGP. With respect to a tilted fireball and realistic 3+1 dimensional hydrodynamical simulations, a significant direct photon elliptic flow is indeed obtained with a weak external mag-

netic field, which verifies the effect of weak magnetic photon emission.

With the updated hydrodynamical modeling including the weak magnetic photon emission, the field strength at initial time and $\eta_s = 0$ can be estimated. In this work, we find a correct centrality dependence of the extracted eB_y^0 , as it increases towards peripheral collisions. However, at RHIC energies, these magnitudes are several times larger comparing to theoretical expectations. This overestimation, as we mentioned previously, is partly due to the space-time profile of the external magnetic field we have adopted. Besides, triangular moment, which was not considered, can contribute to photon elliptic flow as well.

Weak magnetic photon emission can be generalized to higher order flow harmonics of the direct photons. For instance, in a weak magnetic field, the longitudinally dependent elliptic moment in QGP would generate direct photon v_3^γ , while the longitudinal dynamics of a triangular moment can contribute to v_4^γ , etc. These non-trivial correlations between the longitudinal flow of charged hadrons and the spectrum of direct photons should be studied more systematically in future works, both theoretically and experimentally.

Acknowledgements.—We are grateful for very helpful discussions with Charles Gale and Xu-Guang Huang. This work is supported in part by the NSFC Grants through No. 11975079.

-
- [1] E. Shuryak, *Rev. Mod. Phys.* **89**, 035001 (2017), 1412.8393.
 - [2] W. Busza, K. Rajagopal, and W. van der Schee, *Ann. Rev. Nucl. Part. Sci.* **68**, 339 (2018), 1802.04801.
 - [3] C. Gale, S. Jeon, and B. Schenke, *Int. J. Mod. Phys. A* **28**, 1340011 (2013), 1301.5893.
 - [4] C. Shen and L. Yan, *Nucl. Sci. Tech.* **31**, 122 (2020), 2010.12377.
 - [5] C. Gale, *Nucl. Phys. A* **910-911**, 147 (2013), 1208.2289.
 - [6] K. Reygers, *Experimental overview of electromagnetic probes in ultra-relativistic nucleus-nucleus collisions* (2022), URL <https://arxiv.org/abs/2212.01220>.
 - [7] D. Blau and D. Peresunko, *Particles* **6**, 173 (2023).
 - [8] A. Adare et al. (PHENIX), *Phys. Rev. C* **91**, 064904 (2015), 1405.3940.
 - [9] A. Adare et al. (PHENIX), *Phys. Rev. C* **94**, 064901 (2016), 1509.07758.
 - [10] S. Acharya et al. (ALICE), *Phys. Lett. B* **789**, 308 (2019), 1805.04403.
 - [11] C. Shen, U. W. Heinz, J.-F. Paquet, I. Kozlov, and C. Gale, *Phys. Rev. C* **91**, 024908 (2015), 1308.2111.
 - [12] R. Chatterjee and D. K. Srivastava, *Phys. Rev. C* **79**, 021901 (2009), 0809.0548.
 - [13] C. Gale, J.-F. Paquet, B. Schenke, and C. Shen, *Phys. Rev. C* **105**, 014909 (2022), 2106.11216.
 - [14] J.-F. Paquet, C. Shen, G. S. Denicol, M. Luzum, B. Schenke, S. Jeon, and C. Gale, *Phys. Rev. C* **93**, 044906 (2016), 1509.06738.
 - [15] C. Gale, Y. Hidaka, S. Jeon, S. Lin, J.-F. Paquet, R. D. Pisarski, D. Satow, V. V. Skokov, and G. Vujanovic, *Phys. Rev. Lett.* **114**, 072301 (2015), 1409.4778.
 - [16] V. Skokov, A. Y. Illarionov, and V. Toneev, *Int. J. Mod. Phys. A* **24**, 5925 (2009), 0907.1396.
 - [17] A. Bzdak and V. Skokov, *Phys. Lett. B* **710**, 171 (2012), 1111.1949.
 - [18] V. Voronyuk, V. D. Toneev, W. Cassing, E. L. Bratkovskaya, V. P. Konchakovski, and S. A. Voloshin, *Phys. Rev. C* **83**, 054911 (2011), 1103.4239.
 - [19] W.-T. Deng and X.-G. Huang, *Phys. Rev. C* **85**, 044907 (2012), 1201.5108.
 - [20] D. E. Kharzeev, J. Liao, S. A. Voloshin, and G. Wang, *Prog. Part. Nucl. Phys.* **88**, 1 (2016), 1511.04050.
 - [21] X.-G. Huang, *Rept. Prog. Phys.* **79**, 076302 (2016), 1509.04073.
 - [22] K. Hattori and X.-G. Huang, *Nucl. Sci. Tech.* **28**, 26 (2017), 1609.00747.
 - [23] L. McLerran and V. Skokov, *Nucl. Phys. A* **929**, 184 (2014), 1305.0774.
 - [24] K. Tuchin, *Phys. Rev. C* **88**, 024911 (2013), 1305.5806.
 - [25] U. Gürsoy, D. Kharzeev, and K. Rajagopal, *Phys. Rev. C* **89**, 054905 (2014), 1401.3805.
 - [26] L. Yan and X.-G. Huang (2021), 2104.00831.
 - [27] E. Stewart and K. Tuchin, *Nucl. Phys. A* **1016**, 122308 (2021), 2106.09124.
 - [28] A. Huang, D. She, S. Shi, M. Huang, and J. Liao (2022), 2212.08579.
 - [29] J.-J. Zhang, X.-L. Sheng, S. Pu, J.-N. Chen, G.-L. Peng, J.-G. Wang, and Q. Wang, *Phys. Rev. Res.* **4**, 033138 (2022), 2201.06171.
 - [30] G. Basar, D. Kharzeev, D. Kharzeev, and V. Skokov, *Phys. Rev. Lett.* **109**, 202303 (2012), 1206.1334.
 - [31] A. Bzdak and V. Skokov, *Phys. Rev. Lett.* **110**, 192301 (2013), 1208.5502.
 - [32] B. Müller, S.-Y. Wu, and D.-L. Yang, *Phys. Rev. D* **89**, 026013 (2014), 1308.6568.
 - [33] K. Tuchin, *Phys. Rev. C* **91**, 014902 (2015), 1406.5097.
 - [34] B. G. Zakharov, *Eur. Phys. J. C* **76**, 609 (2016), 1609.04324.
 - [35] J. I. Kapusta and C. Gale, *Finite-temperature field theory: Principles and applications*, Cambridge Monographs on Mathematical Physics (Cambridge University Press, 2011), ISBN 978-0-521-17322-3, 978-0-521-82082-0, 978-0-511-22280-1.
 - [36] J. Berges, K. Reygers, N. Tanji, and R. Venugopalan, *Phys. Rev. C* **95**, 054904 (2017), 1701.05064.
 - [37] J.-P. Blaizot, B. Wu, and L. Yan, *Nucl. Phys. A* **930**, 139 (2014), 1402.5049.
 - [38] B. I. Abelev et al. (STAR), *Phys. Rev. Lett.* **101**, 252301 (2008), 0807.1518.
 - [39] B. Abelev et al. (ALICE), *Phys. Rev. Lett.* **111**, 232302 (2013), 1306.4145.
 - [40] S. Chatterjee and P. Božek, *Phys. Rev. Lett.* **120**, 192301 (2018), 1712.01189.
 - [41] D. Teaney and L. Yan, *Phys. Rev. C* **83**, 064904 (2011), 1010.1876.
 - [42] J. Adam et al. (STAR), *Phys. Lett. B* **784**, 26 (2018), 1804.08647.
 - [43] B. Schenke, S. Jeon, and C. Gale, *Phys. Rev. C* **82**,

- 014903 (2010), 1004.1408.
- [44] B. Schenke, S. Jeon, and C. Gale, Phys. Rev. Lett. **106**, 042301 (2011), 1009.3244.
- [45] P. B. Arnold, G. D. Moore, and L. G. Yaffe, JHEP **11**, 001 (2000), hep-ph/0010177.
- [46] J. Churchill, L. Yan, S. Jeon, and C. Gale, Phys. Rev. C **103**, 024904 (2021), 2008.02902.

SUPPLEMENTAL MATERIAL

For the purpose of illustration, we consider the background medium in terms of the Bjorken flow, namely, a flow pattern with longitudinal expansion which is boost invariant and expansion in transverse directions is neglected. Written in the Milne coordinates (τ, η_s) , four-momentum and the flow four-velocity are

$$\begin{aligned} p^\mu &= (p_T \cosh(Y - \eta_s), p_T \cos \phi_p, p_T \sin \phi_p, p_T \sinh(Y - \eta_s)), \\ u^\mu &= (\cosh \eta_s, 0, 0, \sinh \eta_s), \end{aligned} \quad (10)$$

where Y is the rapidity and p_T the transverse momentum. Accordingly, in presence of an external magnetic field orientated along the y direction, the correction in the quark distribution function owing to a weak magnetic field becomes,

$$f_{\text{EM}} \propto eQ_f B_y \frac{\sinh \eta_s}{\cosh(Y - \eta_s)} n_{\text{eq}} \cos \phi_p, \quad (11)$$

where for simplicity only factors of relevance are kept. There can be small anisotropic perturbations on top of the background medium, which are responsible for the anisotropic flow of the observed charged hadrons. In the similar manner as the tilted fireball, if only a rapidity-odd dipolar perturbation is included, one has

$$n_{\text{eq}} = A_0(\tau, \eta_s, p_T, Y) + A_1(\tau, \eta_s, p_T, Y) \cos \phi_p, \quad (12)$$

where the explicit dependence in the functions A_0 and A_1 has been given. Note that, A_0 should be an even function of rapidity as it is related to the particle yields, while A_1 is an odd function in Y . Substitute back to Eq. (11), one has

$$\begin{aligned} f_{\text{EM}} &\propto QB_y \frac{\tau_R}{T} \frac{\sinh \eta_s}{\cosh(y - \eta_s)} (A_0 + A_1 \cos \phi_p) \cos \phi_p \\ &= QB_y \frac{\tau_R}{T} \frac{\sinh \eta_s}{\cosh(y - \eta_s)} \left[\frac{A_1}{2} + A_0 \cos \phi + \frac{A_1}{2} \cos 2\phi \right]. \end{aligned} \quad (13)$$

Since the spectrum of the weak magnetic photon emission is proportional to a space-time integral with respect to f_{EM} , Eq. (13) already implies that $v_2^{\text{EM}} = 0.5$. Since the direct photons in experiments are measured in a symmetric rapidity window, $Y \in [-Y_M, Y_M]$, in the brackets in Eq. (13) the terms that is symmetric in rapidity ($A_0 \cos \phi_p$) should vanish, there is no extra v_1^{EM} contribution. This also explains why we only consider the rapidity-odd dipolar moment in this work.